Polarization sensitive elements fabricated by femtosecond laser nanostructuring of glass [Invited]

Martynas Beresna,* Mindaugas Gecevičius, and Peter G. Kazansky

Optoelectronics Research Centre, University of Southampton, SO17 1BJ, Southampton, UK
**mxb@orc.soton.ac.uk*

Abstract: We review recent progress in application of femtosecond laser nanostructuring of fused silica. The tight control of nanostructures' properties through writing parameters is demonstrated implementing elements with unique optical properties, which can be widely used in material processing, microscopy, optical trapping and manipulation.

OCIS codes: (260.0260) Physical optics; (320.2250) Femtosecond phenomena.

References and links

1. R. R. Gattass and E. Mazur, "Femtosecond laser micromachining in transparent materials," Nat. Photonics **2**(4), 219–225 (2008).
2. W. J. Yang, P. G. Kazansky, and Y. P. Svirko, "Non-reciprocal ultrafast laser writing," Nat. Photonics **2**(2), 99–104 (2008).
3. K. M. Davis, K. Miura, N. Sugimoto, and K. Hirao, "Writing waveguides in glass with a femtosecond laser," Opt. Lett. **21**(21), 1729–1731 (1996).
4. J. W. Chan, T. Huser, S. Risbud, and D. M. Krol, "Structural changes in fused silica after exposure to focused femtosecond laser pulses," Opt. Lett. **26**(21), 1726–1728 (2001).
5. Y. Bellouard, A. Said, M. Dugan, and P. Bado, "Fabrication of high-aspect ratio, micro-fluidic channels and tunnels using femtosecond laser pulses and chemical etching," Opt. Express **12**(10), 2120–2129 (2004).
6. A. Marcinkevi Ius, S. Juodkazis, M. Watanabe, M. Miwa, S. Matsuo, H. Misawa, and J. Nishii, "Femtosecond laser-assisted three-dimensional microfabrication in silica," Opt. Lett. **26**(5), 277–279 (2001).
7. Y. Bellouard, M. Dugan, A. A. Said, and P. Bado, "Thermal conductivity contrast measurement of fused silica exposed to low-energy femtosecond laser pulses," Appl. Phys. Lett. **89**(16), 161911 (2006).
8. R. Osellame, S. Taccheo, M. Marangoni, R. Ramponi, P. Laporta, D. Polli, S. De Silvestri, and G. Cerullo, "Femtosecond writing of active optical waveguides with astigmatically shaped beams," J. Opt. Soc. Am. B **20**(7), 1559–1567 (2003).
9. C. Hnatovsky, R. S. Taylor, E. Simova, P. P. Rajeev, D. M. Rayner, V. R. Bhardwaj, and P. B. Corkum, "Fabrication of microchannels in glass using focused femtosecond laser radiation and selective chemical etching," Appl. Phys., A Mater. Sci. Process. **84**(1-2), 47–61 (2006).
10. Y. Bellouard, A. A. Said, and P. Bado, "Integrating optics and micro-mechanics in a single substrate: a step toward monolithic integration in fused silica," Opt. Express **13**(17), 6635–6644 (2005).
11. Y. Shimotsuma, P. G. Kazansky, J. Qiu, and K. Hirao, "Self-organized nanogratings in glass irradiated by ultrashort light pulses," Phys. Rev. Lett. **91**(24), 247405 (2003).
12. R. Taylor, C. Hnatovsky, and E. Simova, "Applications of femtosecond laser induced self-organized planar nanocracks inside fused silica glass," Laser Photonics Rev. **2**(1-2), 26–46 (2008).
13. J. D. Mills, P. G. Kazansky, E. Bricchi, and J. J. Baumberg, "Embedded anisotropic microreflectors by femtosecond-laser nanomachining," Appl. Phys. Lett. **81**(2), 196–198 (2002).
14. W. J. Cai, A. R. Libertun, and R. Piestun, "Polarization selective computer-generated holograms realized in glass by femtosecond laser induced nanogratings," Opt. Express **14**(9), 3785–3791 (2006).
15. K. Mishchik, G. Cheng, G. Huo, I. M. Burakov, C. Mauclair, A. Mermillod-Blondin, A. Rosenfeld, Y. Ouerdane, A. Boukenter, O. Parriaux, and R. Stoian, "Nanosize structural modifications with polarization functions in ultrafast laser irradiated bulk fused silica," Opt. Express **18**(24), 24809–24824 (2010).
16. E. N. Glezer, M. Milosavljevic, L. Huang, R. J. Finlay, T. H. Her, J. P. Callan, and E. Mazur, "Three-dimensional optical storage inside transparent materials," Opt. Lett. **21**(24), 2023–2025 (1996).
17. S. Juodkazis, H. Misawa, T. Hashimoto, E. G. Gamaly, and B. Luther-Davies, "Laser-induced microexplosion confined in a bulk of silica: Formation of nanovoids," Appl. Phys. Lett. **88**(20), 201909 (2006).
18. C. Hnatovsky, R. S. Taylor, P. P. Rajeev, E. Simova, V. R. Bhardwaj, D. M. Rayner, and P. B. Corkum, "Pulse duration dependence of femtosecond-laser-fabricated nanogratings in fused silica," Appl. Phys. Lett. **87**(1), 014104 (2005).
19. W. J. Yang, E. Bricchi, P. G. Kazansky, J. Bovatsek, and A. Y. Arai, "Self-assembled periodic sub-wavelength structures by femtosecond laser direct writing," Opt. Express **14**(21), 10117–10124 (2006).

#150177 - $15.00 USD Received 29 Jun 2011; revised 28 Jul 2011; accepted 28 Jul 2011; published 29 Jul 2011

20. V. R. Bhardwaj, E. Simova, P. P. Rajeev, C. Hnatovsky, R. S. Taylor, D. M. Rayner, and P. B. Corkum, "Optically produced arrays of planar nanostructures inside fused silica," Phys. Rev. Lett. **96**(5), 057404 (2006).
21. M. Lancry, F. Brisset, and B. Poumellec, "In the Heart of Nanogratings Made up During Femtosecond Laser Irradiation," in *Bragg Gratings, Photosensitivity, and Poling in Glass Waveguides*, OSA Technical Digest (CD) (Optical Society of America, 2010), BWC3.
22. C. Hnatovsky, R. S. Taylor, E. Simova, V. R. Bhardwaj, D. M. Rayner, and P. B. Corkum, "Polarization-selective etching in femtosecond laser-assisted microfluidic channel fabrication in fused silica," Opt. Lett. **30**(14), 1867–1869 (2005).
23. Y. Bellouard, E. Barthel, A. A. Said, M. Dugan, and P. Bado, "Scanning thermal microscopy and Raman analysis of bulk fused silica exposed to low-energy femtosecond laser pulses," Opt. Express **16**(24), 19520–19534 (2008).
24. E. Bricchi and P. G. Kazansky, "Extraordinary stability of anisotropic femtosecond direct-written structures embedded in silica glass," Appl. Phys. Lett. **88**(11), 111119 (2006).
25. Y. Shimotsuma, M. Sakakura, P. G. Kazansky, M. Beresna, J. R. Qiu, K. Miura, and K. Hirao, "Ultrafast manipulation of self-assembled form birefringence in glass," Adv. Mater. (Deerfield Beach Fla.) **22**(36), 4039–4043 (2010).
26. E. Bricchi, B. G. Klappauf, and P. G. Kazansky, "Form birefringence and negative index change created by femtosecond direct writing in transparent materials," Opt. Lett. **29**(1), 119–121 (2004).
27. L. Sudrie, M. Franco, B. Prade, and A. Mysyrewicz, "Writing of permanent birefringent microlayers in bulk fused silica with femtosecond laser pulses," Opt. Commun. **171**(4-6), 279–284 (1999).
28. P. G. Kazansky, H. Inouye, T. Mitsuyu, K. Miura, J. Qiu, K. Hirao, and F. Starrost, "Anomalous anisotropic light scattering in Ge-doped silica glass," Phys. Rev. Lett. **82**(10), 2199–2202 (1999).
29. N. F. Borrelli, C. M. Smith, J. J. Price, and D. C. Allan, "Polarized excimer laser-induced birefringence in silica," Appl. Phys. Lett. **80**(2), 219–221 (2002).
30. M. Ams, G. D. Marshall, and M. J. Withford, "Study of the influence of femtosecond laser polarisation on direct writing of waveguides," Opt. Express **14**(26), 13158–13163 (2006).
31. S. M. Eaton, H. B. Zhang, P. R. Herman, F. Yoshino, L. Shah, J. Bovatsek, and A. Arai, "Heat accumulation effects in femtosecond laser-written waveguides with variable repetition rate," Opt. Express **13**(12), 4708–4716 (2005).
32. R. Buividas, L. Rosa, R. Sliupas, T. Kudrius, G. Slekys, V. Datsyuk, and S. Juodkazis, "Mechanism of fine ripple formation on surfaces of (semi)transparent materials via a half-wavelength cavity feedback," Nanotechnology **22**(5), 055304 (2011).
33. L. Sudrie, A. Couairon, M. Franco, B. Lamouroux, B. Prade, S. Tzortzakis, and A. Mysyrowicz, "Femtosecond laser-induced damage and filamentary propagation in fused silica," Phys. Rev. Lett. **89**(18), 186601 (2002).
34. D. G. Papazoglou, I. Zergioti, and S. Tzortzakis, "Plasma strings from ultraviolet laser filaments drive permanent structural modifications in fused silica," Opt. Lett. **32**(14), 2055–2057 (2007).
35. M. Beresna, P. G. Kazansky, T. Taylor, and A. Kavokin, "Freezing ultrashort light pulses by exciton-polariton interference in glass," in *CLEO: Science and Innovations (CLEO: S and I),* (Baltimore, Maryland, 2011), p. CTuAA4.
36. D. Wortmann, J. Gottmann, N. Brandt, and H. Horn-Solle, "Micro- and nanostructures inside sapphire by fs-laser irradiation and selective etching," Opt. Express **16**(3), 1517–1522 (2008).
37. Y. Shimotsuma, K. Hirao, J. R. Qiu, and P. G. Kazansky, "Nano-modification inside transparent materials by femtosecond laser single beam," Mod. Phys. Lett. B **19**(5), 225–238 (2005).
38. E. Bricchi, J. D. Mills, P. G. Kazansky, B. G. Klappauf, and J. J. Baumberg, "Birefringent Fresnel zone plates in silica fabricated by femtosecond laser machining," Opt. Lett. **27**(24), 2200–2202 (2002).
39. N. Kitaura, S. Ogata, and Y. Mori, "Spectrometer employing a micro-Fresnel lens," Opt. Eng. **34**(2), 584–588 (1995).
40. M. T. Li, J. A. Wang, L. Zhuang, and S. Y. Chou, "Fabrication of circular optical structures with a 20 nm minimum feature size using nanoimprint lithography," Appl. Phys. Lett. **76**(6), 673–675 (2000).
41. J. Canning, K. Sommer, S. Huntington, and A. Carter, "Silica-based fibre Fresnel lens," Opt. Commun. **199**(5-6), 375–381 (2001).
42. W. Watanabe, D. Kuroda, K. Itoh, and J. Nishii, "Fabrication of Fresnel zone plate embedded in silica glass by femtosecond laser pulses," Opt. Express **10**(19), 978–983 (2002).
43. M. Beresna and P. G. Kazansky, "Polarization diffraction grating produced by femtosecond laser nanostructuring in glass," Opt. Lett. **35**(10), 1662–1664 (2010).
44. I. Richter, P. C. Sun, F. Xu, and Y. Fainman, "Design considerations of form birefringent microstructures," Appl. Opt. **34**(14), 2421–2429 (1995).
45. E. Hasman, Z. Bomzon, A. Niv, G. Biener, and V. Kleiner, "Polarization beam-splitters and optical switches based on space-variant computer-generated subwavelength quasi-periodic structures," Opt. Commun. **209**(1-3), 45–54 (2002).
46. M. Beresna, M. Gecevicius, P. G. Kazansky, and T. Gertus, "Radially polarized optical vortex converter created by femtosecond laser nanostructuring of glass," Appl. Phys. Lett. **98**(20), 201101 (2011).
47. S. Quabis, R. Dorn, M. Eberler, O. Glockl, and G. Leuchs, "Focusing light to a tighter spot," Opt. Commun. **179**(1-6), 1–7 (2000).
48. R. Dorn, S. Quabis, and G. Leuchs, "Sharper focus for a radially polarized light beam," Phys. Rev. Lett. **91**(23), 233901 (2003).
49. B. Hao and J. Leger, "Experimental measurement of longitudinal component in the vicinity of focused radially polarized beam," Opt. Express **15**(6), 3550–3556 (2007).

#150177 - $15.00 USD Received 29 Jun 2011; revised 28 Jul 2011; accepted 28 Jul 2011; published 29 Jul 2011

50. D. P. Biss and T. G. Brown, "Polarization-vortex-driven second-harmonic generation," Opt. Lett. **28**(11), 923–925 (2003).
51. S. Carrasco, B. E. A. Saleh, M. C. Teich, and J. T. Fourkas, "Second- and third-harmonic generation with vector Gaussian beams," J. Opt. Soc. Am. B **23**(10), 2134–2141 (2006).
52. D. P. Biss, K. S. Youngworth, and T. G. Brown, "Dark-field imaging with cylindrical-vector beams," Appl. Opt. **45**(3), 470–479 (2006).
53. Q. W. Zhan, "Evanescent Bessel beam generation via surface plasmon resonance excitation by a radially polarized beam," Opt. Lett. **31**(11), 1726–1728 (2006).
54. Y. Liu, D. Cline, and P. He, "Vacuum laser acceleration using a radially polarized CO2 laser beam," Nucl. Instrum. Methods Phys. Res. Sect. A **424**, 296–303 (1999).
55. Q. W. Zhan and J. R. Leger, "Focus shaping using cylindrical vector beams," Opt. Express **10**(7), 324–331 (2002).
56. W. B. Chen and Q. W. Zhan, "Three-dimensional focus shaping with cylindrical vector beams," Opt. Commun. **265**(2), 411–417 (2006).
57. H. F. Wang, L. P. Shi, B. Lukyanchuk, C. Sheppard, and C. T. Chong, "Creation of a needle of longitudinally polarized light in vacuum using binary optics," Nat. Photonics **2**(8), 501–505 (2008).
58. V. G. Niziev and A. V. Nesterov, "Influence of beam polarization on laser cutting efficiency," J. Phys. D Appl. Phys. **32**(13), 1455–1461 (1999).
59. J. A. Davis, D. E. McNamara, D. M. Cottrell, and T. Sonehara, "Two-dimensional polarization encoding with a phase-only liquid-crystal spatial light modulator," Appl. Opt. **39**(10), 1549–1554 (2000).
60. R. Yamaguchi, T. Nose, and S. Sato, "Liquid-crystal polarizers with axially symmetrical properties," Jpn. J. Appl. Phys. **28**(Part 1, No. 9), 1730–1731 (1989).
61. Z. Bomzon, V. Kleiner, and E. Hasman, "Formation of radially and azimuthally polarized light using space-variant subwavelength metal stripe gratings," Appl. Phys. Lett. **79**(11), 1587–1589 (2001).

1. Introduction

In recent years, femtosecond lasers have become a unique tool for three dimensional optical material engineering with the ability to process transparent materials within a confined volume and with nanometer-scale precision [1,2]. Silica glass with femtosecond laser induced properties such as refractive index increase [3,4], selective etching [5,6], thermal conductivity modification [7] has been investigated from the advent of ultrafast direct writing, with applications ranging from integrated optics [8] to micro-fluidics [9] and micro-mechatronics [10]. Over a decade ago a peculiar self-assembling behavior, which manifests as a nanograting formed in the femtosecond laser irradiated volume, was observed in silica glass [11]. Since then, numerous applications of nanogratings have been demonstrated [12] including anisotropic microreflectors [13], polarization sensitive holograms [14] and waveguides [15]. In this review we focus on polarization controlling devices written in fused silica with self-assembled nanograting.

2. Nanograting Properties

Depending on the fluence, femtosecond laser irradiation can produce three types of modification in fused silica: isotropic refractive index increase [3], nanogratings [11] and voids [16,17]. However, all three types can be clearly observed only for pulses shorter than 200 fs [18]. At longer pulses nanogratings appear even at relatively low fluencies, just above a permanent modification threshold. Femtosecond laser induced nanogratings possess two periodicities: perpendicular to the polarization and along light propagation direction [19]. The first grating has a period smaller than the wavelength of light in the range of 100-300 nm depending on experimental conditions (Fig. 1). Despite some works relate this period only to the wavelength [20], in fact it depends in more complex way on a set of parameters such as wavelength and pulse energy [19]. The second period is growing from the head of the structure to the tail with the initial period close to the light wavelength (lambda) in the material (refractive index n), i.e. λ_0 / n. Recent studies suggest that the nanoplanes of the structure consists of a porous material [21] indicating possible glass decomposition during the irradiation of silica glass.

#150177 - $15.00 USD Received 29 Jun 2011; revised 28 Jul 2011; accepted 28 Jul 2011; published 29 Jul 2011

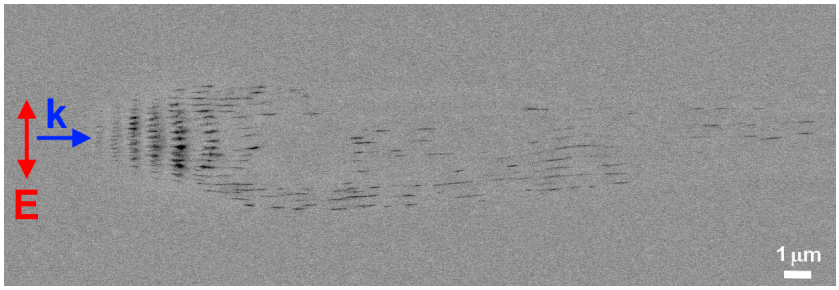

Fig. 1. Cross-section of the nanograting induced in fused silica with femtosecond laser. Two periodicities can be distinguished; one along light propagation **k** and another along the electric field direction **E.**

The nanogratings are able to self-replicate over the distances much larger than the spot size of the writing beam. The experiments suggest that the structure imprinted earlier provides an initial "seeding" conditions during the formation of the self-organized period assembly in the adjacent region [19]. This property affects the etching rates of the irradiated regions [22]. However, recent study indicates that this is not always the case [23]. Additionally nanogratings exhibit extraordinary thermal stability and sustain the temperatures over 1000°C [24]. On the other hand, femtosecond laser pulses with different polarization can completely overwrite modified regions, enabling to explore nanogratings as a rewritable optical medium [12,25].

The predominant way of nanograting characterization is the analysis of the structure under scanning electron microscope [19]. Despite its straightforwardness, the method restricts characterization of the femtosecond laser induced anisotropy to the measurements of the nanograting period. Moreover, it often requires additional post-processing efforts such as sample polishing and etching in fluoric acid. The alternative, nondestructive way of the anisotropic structure's characterization is quantitative birefringence measurements, providing the information about the dependence of induced modification on writing parameters such as fluence, repetition rate, numerical aperture, etc.

3. Form Birefringence

The effect of form birefringence, unlike intrinsic birefringence due to anisotropy of oriented molecules, manifests itself due to alignment of submicroscopic rodlets or platelets [26]. The light polarized parallel to the interfaces experiences larger refractive index and as a result phase difference for two perpendicular polarizations is acquired. The strength of the birefringence can be controlled by periodicity and material composition of the microstructure. Refractive indices of nanograting for ordinary n_o and extraordinary n_e wave are:

$$n_e = \sqrt{\frac{n_1^2 n_2^2}{f_f n_2^2 + (1-f_f) n_1^2}},$$

$$n_o = \sqrt{f_f n_1^2 + (1-f_f) n_2^2},$$

where f_f - filling factor, n_1 and n_2 are refractive indices for platelets constituting the grating. One can see, that

$$n_e^2 - n_o^2 = -\frac{f_f (1-f_f)(n_1^2 - n_2^2)^2}{f_f n_2^2 + (1-f_f) n_1^2} \le 0,$$

#150177 - $15.00 USD Received 29 Jun 2011; revised 28 Jul 2011; accepted 28 Jul 2011; published 29 Jul 2011

i. e. the nanograting always behaves as a negative uniaxial crystal. Typical value of $n_e - n_o$ is $-(2\text{-}4 \times 10^{-3})$ [24]. For comparison, quartz crystal is a positive uniaxial crystal and $n_e - n_o = 9 \times 10^{-3}$. It is worth to note that aligned rodlets produce positive birefringence.

Birefringent modification can be characterized by two parameters: the retardance and the azimuth of the slow axis. On the other hand, they can be independently controlled during the writing experiment as the retardance is a function of fluence and the azimuth of the slow axis is defined by polarization.

Observation of birefringence which could be controlled by polarization of femtosecond IR laser beam was first reported by Sudrie et al [27]. It should be noticed that in these experiments the femtosecond laser induced anisotropy was reported to exhibit positive birefringence. Simultaneously, a peculiar scattering with propeller like shape oriented perpendicular to the laser beam polarization was observed in Ge doped silica glass [28]. It was suggested that aligned subwavelength structures are responsible for this scattering. The experimental observation by Sudrie et al. could be explained by well-known anisotropy due to light induced anisotropic bonds rearrangement (light induced anisotropy) [29]. Knowing that the nanograting always acts as a negative uniaxial crystal these experiments did not suggested presence of the subwavelength structure. Alternatively, experimental error in this paper could be blamed for the sign of birefringence mismatch. All further experiments confirmed the presence of negative birefringence. Discovery of the nanograting produced in the bulk of the material provided an appropriate explanation for the both effects: anomalous scattering and birefringence. Under certain conditions this type of glass modification can be an undesirable effect. As revealed from the studies of the glass modification dependence on the pulse duration, above a certain pulse duration (~200 fs) smooth refractive index increase cannot be achieved [18]. If waveguides are to be written using relatively long pulses >200 fs, they potentially can be polarization sensitive, additionally, some losses can also occur due to nanograting formation [30]. However, at megahertz repetition rates birefringence is strongly reduced, probably due to heat accumulation effects [31]. Despite two theories proposed, the nanograting formation mechanism is still under discussion [11,20,32]. One, adopted from the conventional theory of laser induced surface ripples formation, relies on the interference of bulk electron plasma waves with the incident light [11], while the other attempts to explain the subwavelength structure formation by nanoplasmas [20]. Both theories require relatively high density plasma for nanograting formation, which contradicts predicted [33] and directly measured [34] values of plasma concentration. Recently, alternative theory on nanograting formation based on exciton-polariton self-organization was proposed, which quantitatively explain fine features of the nanogratings, such as two periods [35]. Another open question is a possibility to induce nanogratings in other materials. Currently, nanogratings were observed only in silica glass and several crystalline materials (sapphire [36], tellurium oxide [37]).

4. Birefringent Devices

4.1 Fresnel Zone Plate

One of the first diffractive elements fabricated by means of femtosecond direct writing was a birefringent Fresnel zone plate [38]. Such elements are attractive as optical components due to their compactness and focusing abilities [39]. However, traditional methods of fabrication are based on either lithographic [40] or etching techniques [41], which require costly equipment. The femtosecond direct writing process offers advantages compared with current zone plate fabrication processes because it is a one-step procedure and has the potential for creating polarization-sensitive, integrated multilens systems in three dimensions.

The Fresnel zone plate consists of a series (or zones) of concentric rings whose outer radius R_m is determined by the following equation:

#150177 - $15.00 USD Received 29 Jun 2011; revised 28 Jul 2011; accepted 28 Jul 2011; published 29 Jul 2011

$$R_m = \sqrt{mf\lambda},$$

where m is the number of a respective Fresnel zone and f is the primary focal length.

Figure 2 demonstrates a lens inscribed in a slab of fused silica by selective covering odd-numbered zones with birefringent modification. The lens fabrication was performed with a regeneratively amplified, mode-locked Ti:Sapphire laser delivering 150 fs pulses at 200 kHz repetition rate at 850 nm. The light was focused with 50 × (N. A. 0.55) objective into a fused silica plate at a 0.5 mm depth.

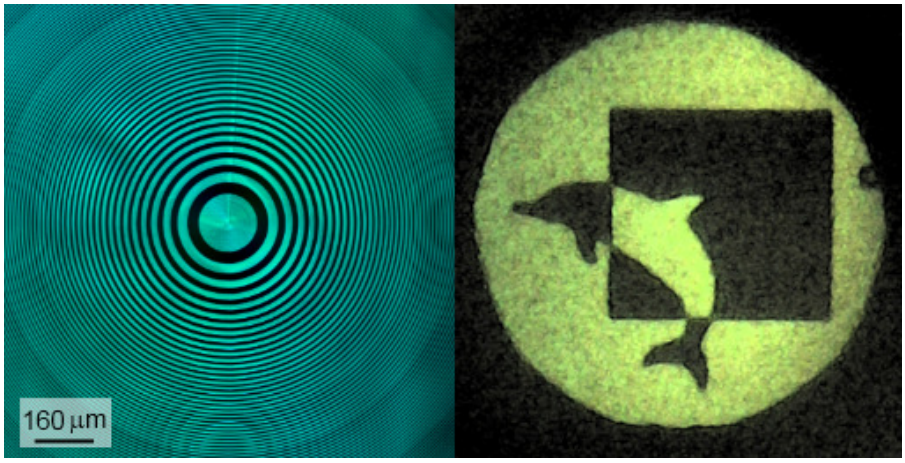

Fig. 2. (Left) Femtosecond laser inscribed Fresnel zone plate, blue regions corresponds to laser processed regions. (Right) Image of the University of Southampton logo projected onto the CCD camera with embedded Fresnel zone plate.

The maximum measured efficiency for this lens, derived as the ratio of a power in each primary focus to the total power incident on the zone plates, was 39%, which is close to the maximum efficiency predicted by theory (about 40%) for a zone plate behaving as a phase lens. For comparison in the case of absorbing zone plates, only 10% efficiency is predicted. This clearly indicates that the focusing properties of this lens were mainly attributed to the variations of refractive index but not amplitude, what could be expected due to scattering on the modified regions. This could explain low efficiency of Fresnel zone plate reported by Watanabe et al [42].

As a result of strong birefringence of the laser induced modification, the lens efficiency largely depends on polarization of incident light and varies by as much as a factor of 6 for orthogonal polarizations. In cross polarizers this lens works as amplitude Fresnel plate. Even when focusing unpolarized light, at the focus the light will be partially polarized. This effect may be useful for integrated optical circuits or micro-electro-mechanical systems applications that require both focusing and polarization sensitivity.

4.2 Polarization Diffraction Grating

Another example of polarization diffractive optical elements is a polarization diffraction grating [43]. Instead of modulating phase or amplitude of the element, one can impose a periodic modulation on the slow axis of the birefringent material [44]. After propagating through the grating, light becomes periodically modulated in a polarization state. If the grating is following the law [45]:

$$\theta(x) = -\left.\frac{\pi x}{d}\right|_{\mathrm{mod}\,\pi},$$

#150177 - $15.00 USD Received 29 Jun 2011; revised 28 Jul 2011; accepted 28 Jul 2011; published 29 Jul 2011

with $\theta(x)$ being the angle of the slow axis, the diffraction has only −1, 0 and 1 orders. The diffraction efficiency depends on the induced retardance R value at the wavelength λ and the state of incident light polarization:

$$\eta_0 = \frac{1}{2}(1+\cos\varphi),$$
$$\eta_{-1,1} = \frac{1}{2}(1-\cos\varphi)\langle E_{in} | RH, LH \rangle^2,$$

where $\varphi = 2\pi R/\lambda$ is the phase shift; E_{in}, RH and LH denote the Jones vectors for incident, right and left polarizations. If the phase shift is equal to π, the zero order, which preserves the incident polarization state, vanishes completely while leaving only right and left handed circularly polarized −1 and 1 diffraction orders. Being sensitive to the handedness of the incident circular polarization, this grating serves as a perfect mean characterizing the polarization state of the incident light.

The polarization grating demonstrated in Fig. 3 was written inside of bulk fused silica using a 200 kHz repetition rate regeneratively amplified diode pumped Yb:KGW (Yb-doped potassium gadolinium tungstate) crystal femtosecond laser operating at λ = 1030 nm. Pulse duration was set to 270 fs and pulse energy was 0.5 μJ. The laser beam was focused via 100 × (N. A. 0.7) Mitutoyo objective into a fused silica plate 70 μm below the surface. Polarization of the incident beam was controlled with an achromatic half-wave plate mounted on a motorized rotation stage. The sample was translated with a computer controlled three-axial stage.

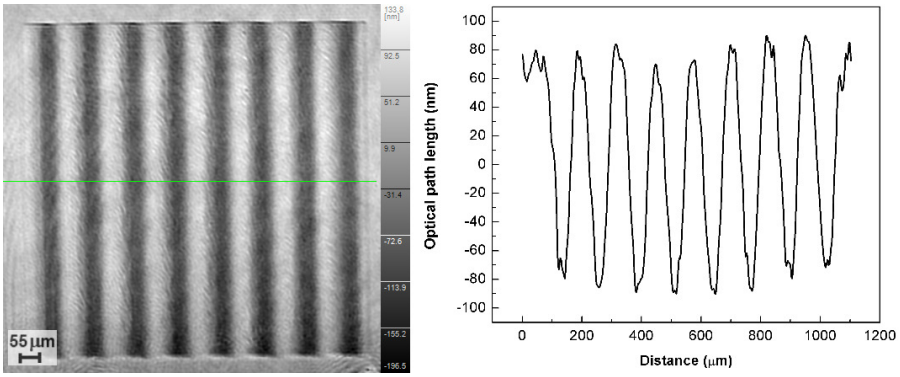

Fig. 3. (Left) Grayscale map representation of birefringent grating phase variation measured with digital holography microscope. (Right) Optical path variation along the green line indicated above.

In the first experiment on writing polarization diffraction grating with femtosecond laser, a moderate retardance of about 80 nm (measured at 515 nm) was induced. As a result, diffraction efficiency into −1 and 1 orders was about 20%.

Recently, a polarization grating size 2 × 2 mm with a 22.5 μm period was written by focusing light with a low NA optics (0.16 N. A.). In this case, a pulse train of 200 kHz with 1.25 μJ pulse energy induced retardance of about 257 nm, which is close to a half-wave for 515 nm. The efficiency of the grating was much higher as compared to that discussed above. More than 80% of the incident light was diffracted into −1 and 1 orders (Fig. 4).

#150177 - $15.00 USD Received 29 Jun 2011; revised 28 Jul 2011; accepted 28 Jul 2011; published 29 Jul 2011

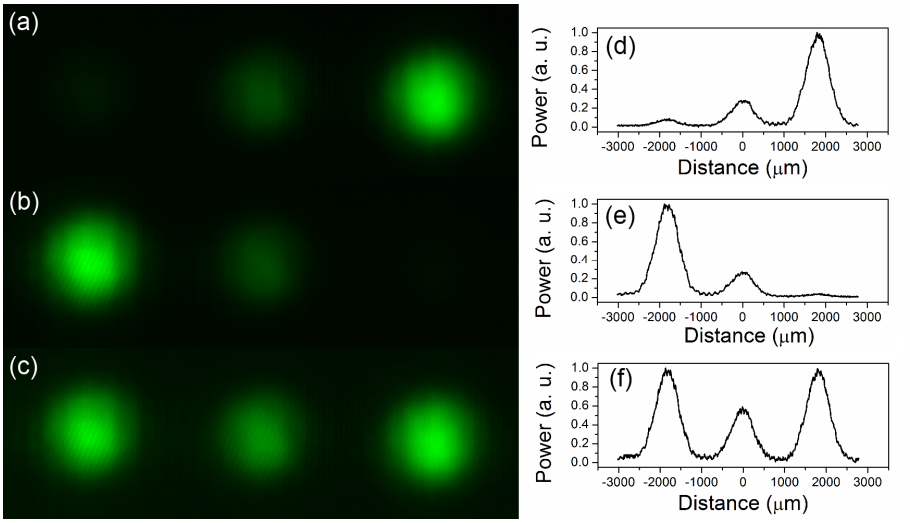

Fig. 4. Far-field diffraction images for circular (right (a) and left (b)) and linear (c) incident polarizations. Respective profiles measured for 515 nm with a beam profile meter: (d,e) diffraction patterns for right and left handed circular polarizations respectively, (f) diffraction pattern for linear polarization.

Sensitivity of polarization grating to incident circular polarization can be exploited for polarimetric measurements.

4.3 Polarization Converter

Another application of femtosecond laser-induced form birefringence is a polarization converter [46]. There is an increasing interest in the exotic polarization modes such as radial or azimuthal polarization. Such beams have attracted recently a significant attention largely because of their unique properties under high numerical aperture (NA) focusing. Numerical calculations have shown that tighter focus spots can be obtained using radial polarization, caused by strong and localized longitudinal field component [47]. This effect has been experimentally confirmed by several groups [48,49] and has already found applications in high resolution imaging such as confocal microscopy, two-photon microscopy, second-harmonic generation microscopy [50], third-harmonic generation microscopy [51], and dark field imaging [52]. Radial polarization also ideally suits for surface plasmon excitation with axially symmetric metal/dielectric structures [53], because plasmon excitation is strongly dependent on excitation polarization. The large longitudinal electric fields generated with radially polarized beams are also explored for particle acceleration [54].

Three-dimensional focus engineering is another application where beams with exotic polarizations can be used. By controlling polarization azimuthal angle φ_0 from the radial direction, a focal field with a transverse flattop profile can be created [55]. Introducing a pupil plane phase or amplitude mask provides additional degrees of freedom and enables extra focal field profile control, so that a highly homogeneous electric field distribution in three dimensions is achieved [56]. Recently, even more exotic focal field distributions, such as an optical “bubble” [56] or optical “needle” [57], have been implemented.

Additionally, high degree of symmetry inherently present in radial/azimuthal polarization leads to efficient interaction with matter without an undesirable anisotropy produced by a linearly polarized light [58]. The main hindrance to a widespread use of such polarization modes is the lack of simple and cost-effective ways to generate them. Currently used methods are mainly based on liquid crystal technology [59,60] or segmented waveplates. However, the low damage threshold restricts the application of liquid crystal based beam converters. Alternatively, polarization converters can be produced by spatially variant subwavelength gratings [61], which would generate azimuthally symmetric polarization from conventional

#150177 - $15.00 USD Received 29 Jun 2011; revised 28 Jul 2011; accepted 28 Jul 2011; published 29 Jul 2011

linearly or circularly polarized Gaussian modes. Photolithography, which is usually used for fabrication of such elements has a limiting resolution that restricts the wavelength of operation to the infrared. In this respect, the nanogratings induced by femtosecond laser irradiation are a perfect choice for devices working in visible and near-infrared. Depending on induced retardance, two types of converters can be constructed. First type is a spatially variant quarter wave plate, which converts an incident circularly polarized beam into a radially or azimuthally polarized optical vortex. Second type, is a spatially variant half-wave plate, which converts incident linear or circular polarization into radial/azimuthal polarization or optical vortex respectively.

Such converters can be efficiently modeled using the Jones matrix formalism. The basic idea behind this model is representing the state of polarization and the effect of an anisotropic device on it by the Jones vector $\vec{E}_{in}$ and the matrix M which contains 2 × 2 elements. The transmitted polarization state $\vec{E}_{out}$ then can be written as:

$$\vec{E}_{out} = M\vec{E}_{in}$$

The matrix for a spatially variant element can be obtained by rotation transformation expressed as follows:

$$M(\theta) = R(-\theta)MR(\theta),$$

where

$$R(\theta) = \begin{pmatrix} \cos(\theta) & \sin(\theta) \\ -\sin(\theta) & \cos(\theta) \end{pmatrix}.$$

The spatially variant quarter wave plate when can be described by the following matrix:

$$M_{qw} = \begin{pmatrix} \cos^2\theta + i\sin^2\theta & (1-i)\cos\theta\sin\theta \\ (1-i)\cos\theta\sin\theta & i\cos^2\theta + \sin^2\theta \end{pmatrix},$$

where $\theta = \phi + \pi/4$ and ϕ is a polar angle in the polar coordinate system. Multiplying a vector describing the left handed circular polarization by this matrix, the following expression is derived:

$$\vec{E}_{azi} = M_{qw}\frac{1}{\sqrt{2}}\begin{pmatrix} 1 \\ i \end{pmatrix} = \begin{pmatrix} -\sin\phi \\ \cos\phi \end{pmatrix} e^{i\phi}e^{i\pi/4}.$$

The first term of the product represents azimuthal polarization while the second term indicates the presence of the orbital angular momentum l = 1. Similar calculations made for the right handed incident polarization yield radial polarization with the orbital momentum l = −1.

For a spatially variant half-wave plate, we get the following Jones matrix expression:

$$M_{hw} = \begin{pmatrix} \cos\phi & \sin\phi \\ \sin\phi & -\cos\phi \end{pmatrix}.$$

Then for the incident horizontally polarized light, the radial polarization emerges:

$$\vec{E}_{rad} = M_{hw}\begin{pmatrix} 0 \\ 1 \end{pmatrix} = \begin{pmatrix} \sin\phi \\ -\cos\phi \end{pmatrix}.$$

#150177 - $15.00 USD Received 29 Jun 2011; revised 28 Jul 2011; accepted 28 Jul 2011; published 29 Jul 2011

Similarly for the incident vertically polarized light, the azimuthal polarization is derived. The superposition of two azimuthally symmetric polarization states can be easily produced by rotating the incident beam polarization with respect to the radially variant half-wave plate. An interesting result follows if a circularly polarized light is transmitted through the same converter:

$$\vec{E}_{vor} = M_{hw}\begin{pmatrix}1\\ i\end{pmatrix} = \begin{pmatrix}\cos\phi + i\sin\phi\\ \sin\phi - i\cos\phi\end{pmatrix} = e^{i\phi}\begin{pmatrix}1\\ -i\end{pmatrix}.$$

As one can see, incident circular polarization changes its handedness and additionally acquires a spatially variant phase factor which is a direct indication of optical vortex presence. As a result, the same converter can be used for generation of azimuthally symmetric polarization states and optical vortices (Fig. 5).

If a converter is designed for 515 nm wavelength, the corresponding retardance values for quarter- and half-wave are 128.75 nm and 257.5 nm. First, a series of experiments were performed to determine a writing regime where such high values of retardance can be achieved. For the experiments we used the same Yb:KGW femtosecond laser system as described in the above paragraph with the repetition rate set to 200 kHz.

In our femtosecond writing setup, the colimated femtosecond beam passes through a half-wave plate and a Glan polarizer (used for controlling the average power). The second half-wave plate, located just before the focusing optics avoiding unwanted polarization distortion, controls polarization of the writing beam. The beam is focused with the relatively low numerical aperture (NA = 0.16-0.35) lenses and objectives, allowing the increased values of induced retardance as a result of an extended Rayleigh length. The sample is mounted onto an XYZ linear air-bearing precise positioning stage (Aerotech Ltd.).

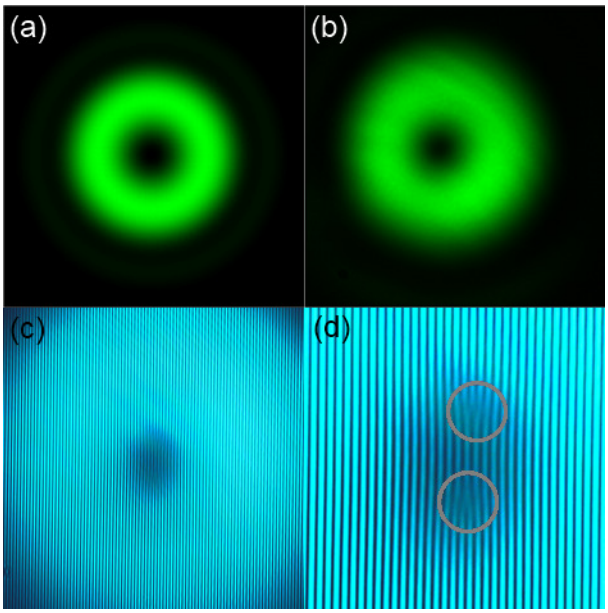

Fig. 5. (a) Modeled and (b) measured vortex intensity profiles, (c) diffraction pattern of two interfering vortices, (d) zoomed central part, red circles indicate 'fork' pattern formed due to phase discontinuity present in the interfering electric field.

The optimum parameters to induce a high retardance were determined by a set of experiments. The structures were written with two different translation speeds (1mm/s and 2mm/s) at energies up to 7.5 μJ and later characterized with a quantitative birefringence measurement system (CRi Abrio) and Olympus BX51 optical microscope. The measured retardance dependence on pulse energy at two different focusing conditions clearly

#150177 - $15.00 USD Received 29 Jun 2011; revised 28 Jul 2011; accepted 28 Jul 2011; published 29 Jul 2011

demonstrates possibility of reaching high retardance values exceeding even half-wave value (258 nm) for 530 nm (Fig. 6). One can see that with lower NA optics, the higher energy is required for forming nanogratings and, as a result, the structures with the same retardance are less uniform. However, the retardance saturates at much higher values, allowing to write a half-wave retardance in a single scan. With 0.35 NA objective severe damage of glass occurs above 3 μJ limiting the induced retardance to 200 nm.

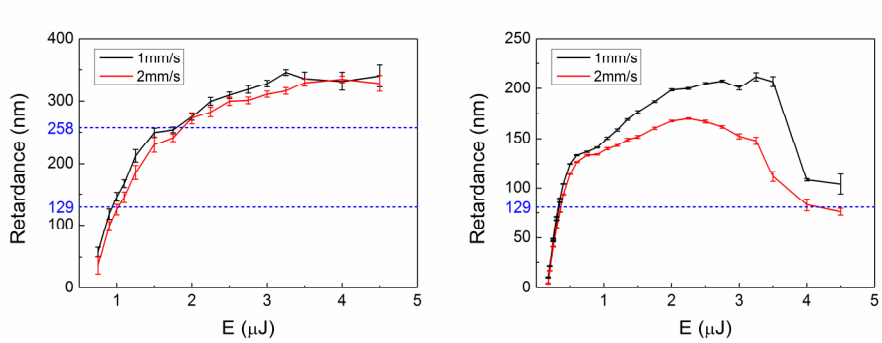

Fig. 6. Retardance values for nanogratings written with 0.16 NA aspheric lens (Left) and 0.35 NA objective (Right) at two translation speeds (1 and 2 mm/s). Dotted lines indicate retardance values of quarter and half wave for 530 nm.

To get the retardance value of a quarter-wave, the light was focused via the objective of NA = 0.35 as this requires less energy that means that the structures are more uniform. For the retardance value of a half-wave, the light was focused via an aspheric lens with NA = 0.16 and the writing speed was 2 mm/s. The converters were recorded by translating the sample in spiral trajectory with the synchronous rotating polarization. The optimized writing process allowed to appreciably reduce the total fabrication time, which in comparison to a previous result was lowered by a factor of 7 (Fig. 7).

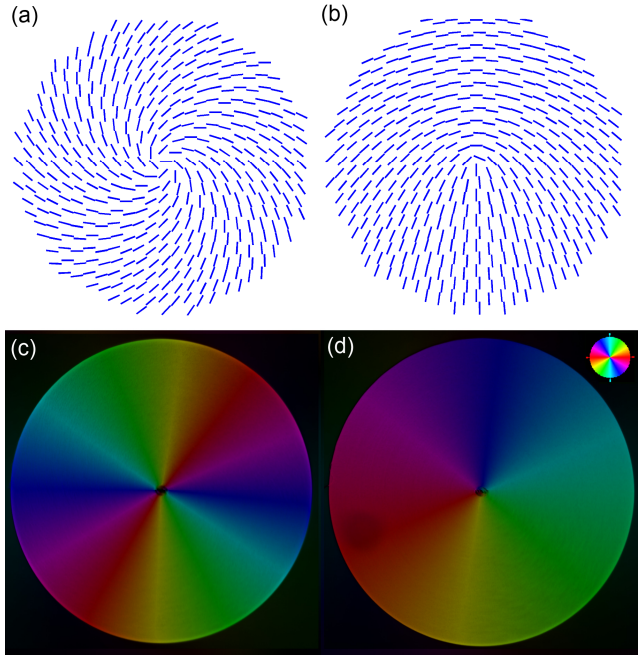

Fig. 7. Schematic drawings of nanogratings distribution in quarter- (a) and half-wave (b) polarization converters. Femtosecond laser written radial polarization converters for circular (c) and linear (d) incident polarizations. The pseudo color indicates direction of the slow axis.

#150177 - $15.00 USD Received 29 Jun 2011; revised 28 Jul 2011; accepted 28 Jul 2011; published 29 Jul 2011

Performance of the converter for circular polarization was investigated with a circularly polarized argon ion laser beam (λ = 514 nm). After passing the quarter-wave retardance converter, the beam was transmitted through a linear polarizer and collected by a CCD camera. For comparison, the respective beam profiles were modeled using the Jones calculus and Fourier propagation (Fig. 8). In the near-field, modelling and measurements produced the propeller shapes typical for the radial polarization. In the far-field, the diffraction distorts this shape producing a peculiar '*s*' shape pattern, though symmetric propeller shape can be restored in the near-field by focusing the beam again.

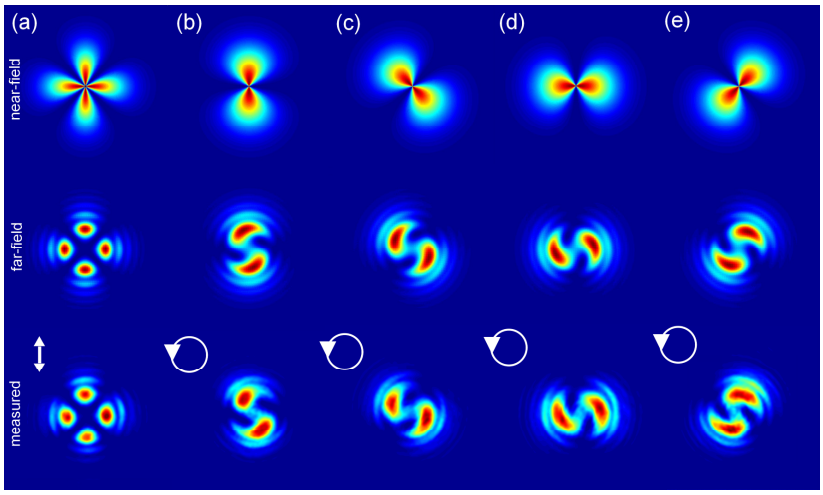

Fig. 8. Modeled near- and far-field (top and middle) and measured (bottom) intensity distributions after the polarization converter for incident linear polarization (a) and for left handed circular polarization (i.e., azimuthal polarization with the orbital angular momentum l = 1 is generated) at different angles of polarizer 0° (b), 45° (c), 90° (d), 135° (e). White arrows indicate incident polarization state.

An azimuthally (radially) polarized vortex with the orbital angular momentum $l = 1$ ($l = -1$) can be considered as a superposition of two circularly polarized beams, one possessing the orbital angular momentum $l = 2$ ($l = -2$) and the other having a plane front. The interference of these two beams after the polarizer (analyser) produces a characteristic '*s*' shape pattern, which was observed in our experiment.

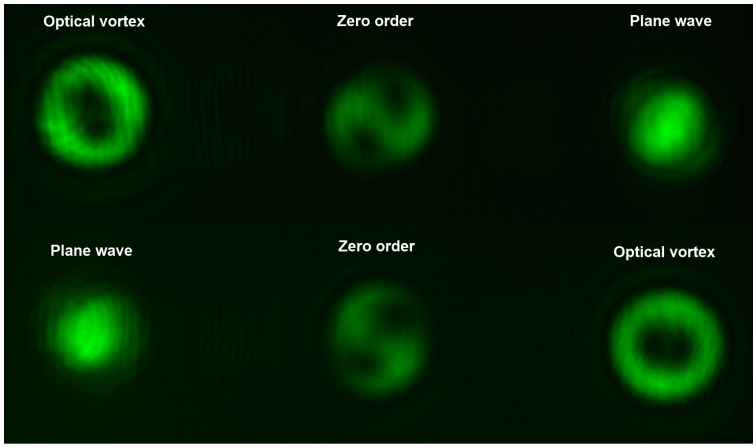

Fig. 9. Diffraction patterns of radially/azimuthally polarized optical vortices produced with the polarization grating discussed in section 4.2.

#150177 - $15.00 USD Received 29 Jun 2011; revised 28 Jul 2011; accepted 28 Jul 2011; published 29 Jul 2011

To visually demonstrate this, we transmitted a radially polarized optical vortex generated with the converter through the polarization grating discussed above (Fig. 9). As this grating works as a circular polarization beam splitter, the incident beam was split into an optical vortex and a plane wave.

Similar procedure was used for testing a half-wave retardance converter. In this case, a radial polarization is produced by the incident linear polarization. As this is a pure radial polarization as opposed to the radially polarized optical vortex described above, the propeller shape is retained even in the far-field (Fig. 10).

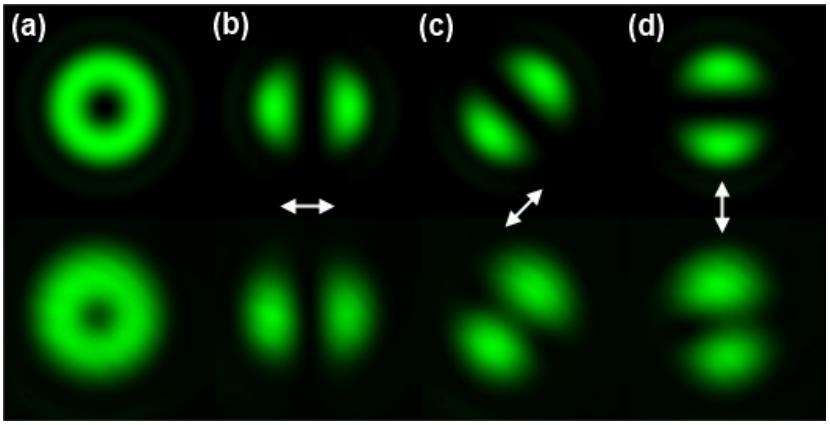

Fig. 10. Modeled (top) and measured (bottom) profiles of generated radial polarization directly after converter (a) and after polarizer (b-d). White arrows indicate transmission axis of the polarizer inserted between the converter and the CCD camera.

4. Conclusions

Femtosecond laser direct writing can be used for a three dimensional nanostructuring of silica glass. The process not only allows fabricating complex optical devices in a single step but also opens new opportunities for precise control of induced birefringence. Potential of this method was demonstrated by implementing several unique polarization-sensitive devices ranging from diffraction gratings to radial polarization and optical vortex converters which could be used for polarimetry, microscopy, and material processing to mention only few.

Acknowledgments

The work was supported by the Engineering and Physical Sciences Research Council (EPSRC Project No. EP/E034802/1) and the project FEMTOPRINT, financed by the European Commission Factories of the Future program (FP7/ NMP/Project No 260103), http://www.femtoprint.eu/.

#150177 - $15.00 USD Received 29 Jun 2011; revised 28 Jul 2011; accepted 28 Jul 2011; published 29 Jul 2011